Vol. 702: 19–38, 2022
https://doi.org/10.3354/meps14210

MARINE ECOLOGY PROGRESS SERIES
Mar Ecol Prog Ser

Published December 8

Microbial-driven impact on aquatic phosphate fluxes in a coastal peatland

Simeon Choo[1,2,*], Olaf Dellwig[3], Janine Wäge-Recchioni[1], Heide N. Schulz-Vogt[1,2]

[1]Department of Biological Oceanography, Leibniz Institute for Baltic Sea Research Warnemünde, 18119 Rostock, Germany
[2]Faculty of Mathematics and Natural Sciences, University of Rostock, 18059 Rostock, Germany
[3]Department of Marine Geology, Leibniz Institute for Baltic Sea Research Warnemünde, 18119 Rostock, Germany

ABSTRACT: Polyphosphate-accumulating microbial mats can influence PO_4^{3-} concentration in the benthic zone. To investigate the role of microbial mats in benthic P cycling, short peat cores including supernatant water from a coastal fen in NE Germany (southern Baltic Sea) were incubated in winter, summer and fall under 3 conditions: *in situ*, elevated temperature and oxygen-depletion. Bottom water PO_4^{3-} concentrations decreased in treatments where a microbial mat had formed (summer and winter) but not in the mat-deficient fall treatment. The mats were densely populated with polyphosphate-rich *Lyngbya* sp. filaments. On the last day of incubation, PO_4^{3-} concentrations in the oxygen-depleted bottom water were lower in the winter (70×) and summer (44×) than in the fall treatment, demonstrating the significant effect of microbial mats on PO_4^{3-} fluxes, even under oxygen-depleted conditions. Mean polyphosphate-P content in the upper 1 cm peat layer of 8 freshly collected winter cores was 2.23 µmol g^{-1} (5% of total P), comprising a noticeable percentage of the P reservoir. Low sediment Fe:P molar ratios among the cores (5.9–6.3) indicated that P-adsorption sites in Fe-P compounds were fairly saturated and had limited efficiency in precipitating additional bottom water PO_4^{3-}. Using known temperature-dependent coefficients for biological systems, we estimate that bottom water PO_4^{3-} concentrations in temperature-elevated cores were reduced by 96% in the presence of a microbial mat. We propose that a microbial mat can take up a large amount of dissolved inorganic P, highlighting its regulatory role in coastal peatland P fluxes under varying environmental conditions.

KEY WORDS: Polyphosphate · *Lyngbya* spp. · Microbial mat · Benthic · Phosphorus cycling · PolyP-accumulating bacteria · Baltic Sea · Cyanobacteria

1. INTRODUCTION

Along the coastline of the southern Baltic Sea, the delivery of dissolved P from the terrestrial domain to the sea is markedly affected by microbial processes and associated redox changes in the surface sediments (Carstensen et al. 2020). Organic matter remineralization is a major driver of PO_4^{3-} release in sediments (Viktorsson et al. 2013). Redox changes in the surface layer also result in either P release from or adsorption to redox-sensitive sediment fractions (McColl 1977, Yu et al. 2017), thereby influencing nutrient fluxes such as PO_4^{3-} at the sediment–water interface. Although organic matter remineralization and factors influencing redox in sedimentary P fluxes in aquatic environments are well-studied (Mortimer 1942, Jensen & Thamdrup 1993, Lake et al. 2007), the significance of polyphosphate (polyP) storage by microbes in the P cycle is still underestimated (Kornberg et al. 1999, Rao et al. 2009, Xie & Jakob 2019). As a polymer comprising numerous orthophosphate molecules linked via high-energy phosphoanhydride bonds (Nocek et al. 2008), polyP is an important intracellular energy and PO_4^{3-} reser-

*Corresponding author: simeon.choo@io-warnemuende.de

Publisher: Inter-Research · www.int-res.com

voir. In prokaryotes, polyP is synthesized and stored in granules, which can be hydrolyzed to orthophosphates or used for the formation of energy-rich compounds such as ADP, ATP, GDP and GTP (Achbergerová & Nahálka 2011).

The P cycle is more complicated than previously imagined due to a limited understanding of the microbial contribution (Dale et al. 2016). Nevertheless, a fair number of studies have proposed the role of microbial P-fixation in sedimentary P cycling. Benthic bacteria have been suggested to influence the P flux across the sediment–water interface and stimulate P regeneration and burial by converting settling organic P to refractory organic P such as inositol hexakisphosphates (Gächter & Meyer 1993, Ingall & Jahnke 1997, Jørgensen et al. 2011). In certain environments, such as the Namibian shelf (Schulz & Schulz 2005), the Black Sea (Schulz-Vogt et al. 2019) and the stratified crater Lake Pavin (Rivas-Lamelo et al. 2017), polyP-accumulating microorganisms possibly play a significant role in P cycling. This could be attributed to their size and ultimately the amount of polyP they can accumulate both in nature (Schulz-Vogt et al. 2019) and in a controlled environment (Comeau et al. 1986, Rubio-Rincón et al. 2017). In a laboratory setting, large filamentous sulfur bacteria of the genus *Beggiatoa* were shown to store polyP during favorable growth conditions and release it as PO_4^{3-} under disadvantageous environmental stimuli; for instance, during anoxic or even sulfidic conditions (Brock & Schulz-Vogt 2011, Langer et al. 2018, Hermans et al. 2019). Furthermore, bloom-forming benthic cyanobacteria such as those of the genus *Lyngbya* are potentially able to accumulate large amounts of polyP (Arthur et al. 2009).

Microbial P cycling has a key role in P turnover in wetlands. Intensively farmed peatlands along the German Baltic coast have been restored over the last few decades, mainly through the practice of long-term rewetting, in an effort to reduce greenhouse gas emissions from degraded peat (Weil et al. 2020). However, peatland rewetting has also led to increased mobilization and input of P to the water column (Zak & Gelbrecht 2007, Lundin et al. 2017), making these sites ideal for investigating the influence of microbial P uptake and release on the P flux at the sediment–water interface. Although the significance of microbial-associated polyP in P recycling is gradually being acknowledged (McMahon & Read 2013, Dale et al. 2016, Li et al. 2019), it is still uncertain whether the PO_4^{3-} concentration in bottom waters is directly affected by microbial PO_4^{3-} uptake and release from the surface sediment layer. The effect of changing environmental conditions such as temperature and oxygen availability on this mechanism is also unclear.

The concept of PO_4^{3-} uptake under oxygen-depleted conditions is still under debate to this day; however, it has been shown that bacteria exist which are able to take up and sequester PO_4^{3-} in both oxic and anoxic sediments (Kerrn-Jespersen & Henze 1993, Goldhammer et al. 2010). In this study, we investigated the influence of mat-forming microbes on the P flux in a coastal peatland (southern Baltic Sea) under *in situ* conditions as well as under elevated temperature and depleted oxygen conditions. Ultimately, our findings shed light on the importance of the microbial layer in mitigating the benthic P flux amid changing environmental conditions.

2. MATERIALS AND METHODS

2.1. General procedure

Preliminary sampling at our study site in a rewetted peatland (see Fig. 1) identified polyP-accumulating microbial mats mainly comprising filamentous cyanobacteria of the genus *Lyngbya*. These were largest in February–June (winter–early summer) and significantly reduced in size in August–November (late summer–fall).

Incubation of short peat cores collected from the study site was carried out firstly in winter in order to determine the effect of the microbial mat on the P flux into the bottom water. This incubation was repeated in early summer when the microbial mat was still present to examine the effect of mat removal and re-establishment on the P flux. Here, the upper 1 cm layer of the peat was removed from the summer cores on Day 2 of the incubation, to test for a potential increase in bottom water PO_4^{3-} concentration via a less inhibited release of porewater PO_4^{3-} due to the reduced presence of the mat. We could also observe if any equilibration of the bottom water PO_4^{3-} concentration occurred after the mat was removed as well as any possible effects of mat re-establishment. As a negative control with conditions similar to the oxygen-depleted winter treatment, a third incubation with samples obtained in fall was carried out under oxygen depletion to determine the effect of a permanently reduced mat on the P flux. Since the oxygen-depleted treatments conducted earlier in winter and summer showed that the presence of a microbial mat was capable of counteracting an increase in bottom water PO_4^{3-} levels via release

from Fe-bound P, we assumed that it was sufficient to only implement the oxygen-depleted treatment in the fall incubation. To relate the decrease of bottom water PO_4^{3-} to sequestration by the microbial mat, the change in the polyP-P content in the surface peat layer was also measured at the start and end of the winter incubation. Accordingly, we examined if *Lyngbya* spp. filaments accumulated polyP in treatments with a microbial mat present (winter and summer).

2.2. Study site

Samples were collected from a coastal fen in Karrendorfer Wiesen, Germany (54° 09′ N, 13° 23′ E) (Fig. 1), a restored peatland covering an area of approx. 3.5 km^2 surrounded by a salt marsh (Bernhardt & Koch 2003, Seiberling & Stock 2009). The low-lying parts of the peatland experience frequent flooding, since a de-embankment in 1993 allowed for the restoration of natural flood dynamics. The fen lies in close proximity to the Baltic Sea (shortest distance: approx. 4 m) and is irregularly flooded, e.g. during storm events. The study site is also frequently inundated with rainwater except during the late summer when precipitation is minimal. The surface layer of the fen comprises a mixture of typical marsh plant debris (e.g. reed stalks, spindly leaves) and peat soil. Temperatures range between 0°C around the end of January and 31°C in late July. From our study data, strong fluctuations in salinity at the site were observed, with 5.1 psu in late January and 18.7 psu in late July.

2.3. Sampling in the field

Short peat cores for the incubation experiments were obtained in winter (February 2020), summer (June 2020) and fall (October 2020) at the study site (Fig. 1). At the time of collection, the mean water temperature, salinity, pH and oxygen readings were 5.9°C, 5.8 psu, pH 7.3, 13.5 mg l^{-1} (winter); 15.2°C, 11.5 psu, pH 5.6, 7.6 mg l^{-1} (summer); and 13.7°C, 7.8 psu, pH 6.9, 10.8 mg l^{-1} (fall). Cores were collected using acrylic tubes, each with a length of 20 cm and an inner diameter of 7 cm. Each core was collected by manual boring of the tube into the peat until a depth of about 10 cm was attained. Both peat

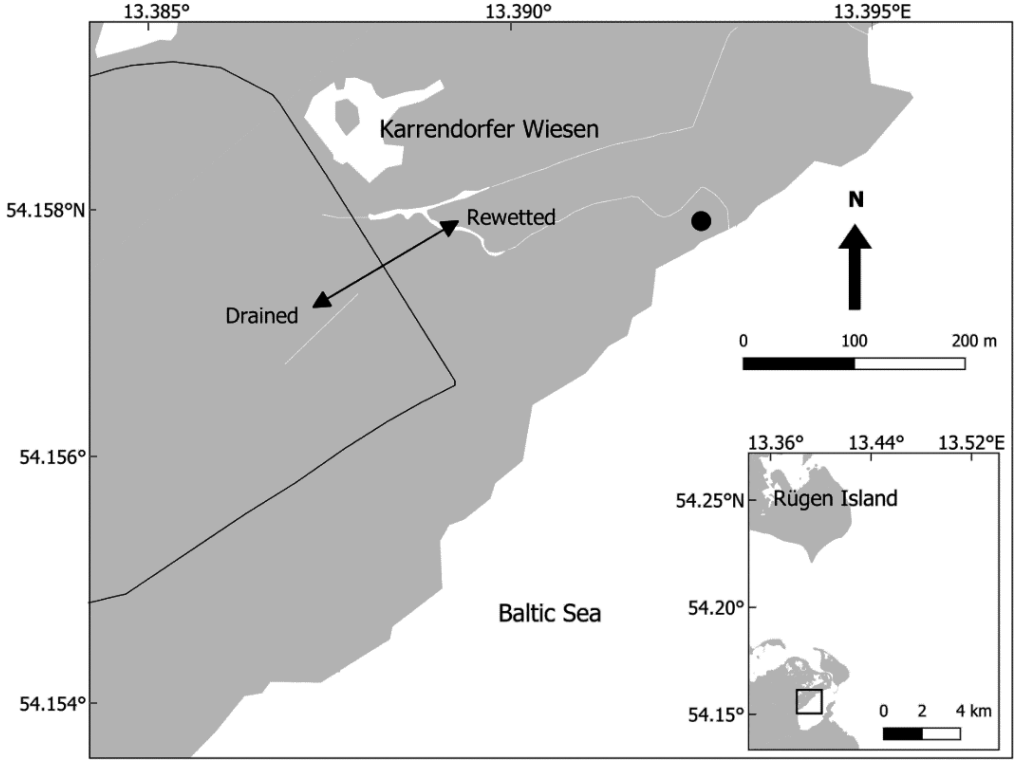

Fig. 1. Sampling area Karrendorfer Wiesen, in the state of Mecklenburg-Western Pomerania, NE Germany. Short cores were collected at a fen peat (black dot) in the rewetted zone. The peat and water depth in the cores ranged from 11–13 and 9–11 cm, respectively, during the study

and supernatant water (here referred to as bottom water) were recovered in the same tube to ensure minimal disturbance of the benthic organisms. Bottom water variables of temperature, dissolved oxygen and conductivity were measured on-site, and salinity was calculated using a Hach HQ40D Portable Multimeter.

For the determination of total P and Fe, 8 additional short peat cores were collected at the sampling site on Day 0 of the winter experiment. The upper 1 cm layer of peat was then hollowed out from each core, homogenized and stored in eight 50 ml Falcon tubes. A sub-sample was collected from each tube and weighed. Each sub-sample was designated as a replicate. The sub-samples were then freeze-dried for 48 h, weighted for water content and homogenized using an agate mortar.

2.4. Incubation experiments and sampling

The short peat cores including bottom water were incubated in INFORS HT Multitron Pro incubators over either 8 or 10 d periods under different treatments (Table 1). Day 0 represented the first day of incubation. The *in situ* temperature refers to the water temperature at the time of core collection. In addition, cores which were part of the '*in situ* + 10°C' treatment were incubated at 10°C higher than the *in situ* temperature. A negative control treatment with a nearly absent bacterial mat was also set up in the fall under oxygen-depleted conditions to illustrate the effect of reduced microbial PO_4^{3-} uptake on bottom water PO_4^{3-} concentration. Each treatment was carried out in triplicate. The *in situ* temperature of each seasonal treatment was as follows: winter, 5°C; summer, 15°C; fall, 5°C. The aerobically treated cores were continually exposed to light during incubation to maintain photosynthetic activity and oxygen production. In order to restrict the growth of photosynthetic organisms within the peat, the outer surface of the core exposing the peat column was wrapped with aluminum foil (Fig. 2). For the oxygen-depleted treatment, pure nitrogen gas (N_2) was bubbled into the water column for 20–25 min to achieve an approximate oxygen concentration of 1.7 mg l^{-1} before the start of the incubation. The oxygen content in these cores

Table 1. Incubation treatments (8–10 days) of short cores collected at Karrendorfer Wiesen in winter, summer and fall in 2020 (n = 3), to investigate the effect of temperature elevation and oxygen depletion on PO_4^{3-} cycling. OX: aerobic; OD: oxygen-depleted; number refers to temperature

Season	Treatment		
	Aerobic, *in situ* temperature	Aerobic, *in situ* temp. +10°C	Oxygen-depleted, *in situ* temperature
Winter	WinterOX5	WinterOX15	WinterOD5
Summer	SummerOX15	SummerOX25	SummerOD15
Fall	–	–	FallOD5 (negative control)

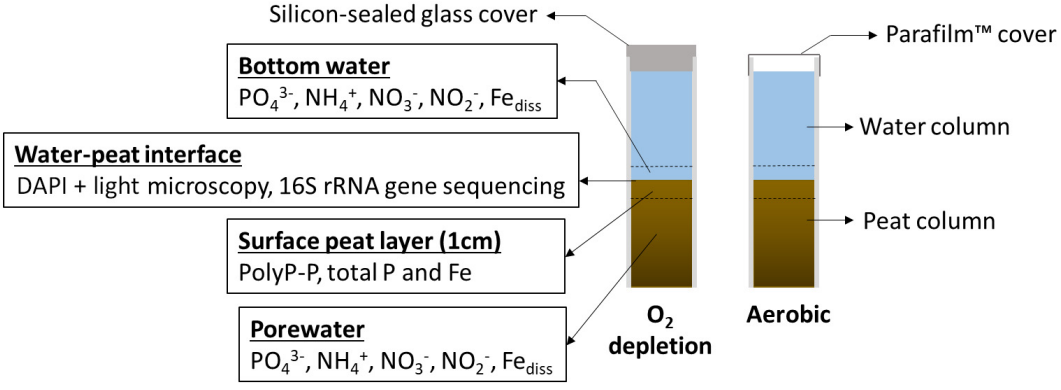

Fig. 2. Core details and parameters measured. Bottom water, porewater, water–peat interface and surface peat layer subsamples were extracted on either a daily or one-time basis from all cores. In the summer treatment cores, the upper 1 cm peat layer was removed on Day 2 of the inclubation to eliminate a significant portion of the microbial mat and trigger the release of porewater PO_4^{3-} to the bottom water. PolyP: polyphosphate; Fe_{diss}: dissolved Fe

was not monitored throughout the incubation period; however, oxygen-depleted conditions were maintained by keeping the cores in complete darkness to inhibit photosynthetic activity. After each daily bottom water sampling using a 15 ml syringe, oxygen-depleted conditions in the cores were preserved by refilling the water column with N_2-bubbled water collected from the sampling site. The top opening of the core was then glass-capped and sealed with industrial-grade silicone sealant to prevent gaseous exchange with the ambient environment. Throughout the incubations, pH in the 3 seasonal treatments ranged from 5.8–7.5. In the summer treatment, cores were incubated in the same way as in the winter and fall treatments, except that the upper 1 cm layer of peat (including the microbial mat) was carefully removed from each core after the bottom water was sampled on Day 2. Three sub-samples of the exposed peat layer from each core were then visualized via light microscopy to check for any remains of a microbial mat.

On Day 0 and the last day, peat sub-samples from cores of the winter treatments were obtained by slicing at depths of 0–0.7 and 0.7–1.4 cm and then homogenized. A total of 2 ml of peat was collected from each homogenized sub-sample for subsequent microscopic and geochemical analyses as well as polyP-P quantification. For determination of dissolved inorganic nutrients and Fe in bottom waters, 12 ml of water was collected daily from each incubation core and filtered through a Whatman® glass microfiber filter (GF/F grade, 25 mm diameter). Prior to collection, the bottom water was homogenized by slight stirring with a flat-surfaced plastic stirrer, which ensured minimal disturbance to the surface peat layer. A 2 ml aliquot was transferred into 2 ml reaction tubes and immediately acidified with concentrated HNO_3 to 2 vol% before storage of the filtered samples for nutrient measurements at −20°C. The nutrient and dissolved Fe concentrations were later corrected for the decreasing water volume in the core.

Porewater samples for nutrients and dissolved Fe (2 ml each) were extracted just below the peat–water interface, at 0.8 and 1.5 cm using rhizons (Seeberg-Elverfeldt et al. 2005; Rhizon CSS 19.21.23F pore size 0.15 µm; Rhizosphere Research Products). Sampling was done on Day 0 and on the last day of incubation and treated in the same way as described for the bottom water samples.

2.5. Dissolved inorganic nutrients

Concentrations of dissolved PO_4^{3-}, ammonium (NH_4^+), nitrate (NO_3^-) and nitrite (NO_2^-) in both bottom water and porewater samples were measured colormetrically (Hansen & Koroleff 1999) by a Seal Analytical QuAAtro constant flow analyzer with a precision of 2.0% for PO_4^{3-} and 3.1% for NO_x (i.e. $NO_3^- + NO_2^-$) (Krause et al. 2021).

2.6. Diffusive PO_4^{3-} fluxes

From the bottom water and porewater PO_4^{3-} values (Table 2), the PO_4^{3-} diffusive fluxes from the surface peat layer into the overlying bottom water were calculated using Fick's First Law. PO_4^{3-} diffusion coefficients were corrected for temperature, salinity and porosity (Boudreau 1997, Berg et al. 1998, Schulz & Zabel 2006). Porosity data was derived according to Flemming & Delafontaine (2000), using the mean moisture content and dry bulk density of the aforementioned 8 peat subsamples.

2.7. Dissolved Fe

The concentration of dissolved Fe (Fe_{diss}) in bottom water and porewater samples was determined by inductively coupled plasma–optical emission spectrometry (ICP-OES; iCAP 7400 Duo, Thermo Fisher Scientific) with a salinity-matched calibration using diluted Atlantic Seawater (OSIL). Scandium (Sc) served as the internal standard to eliminate remaining matrix effects. Precision and trueness of the international reference material SLEW-3 (NRCC) spiked with 0.9 and 3.6 µmol l^{-1} Fe_{diss} were 3.7 and 0.5%, respectively. The Fe_{diss} concentration in the water column was corrected

Table 2. Concentration of PO_4^{3-} at 2 peat depths and resultant diffusive fluxes from the peat into the overlying bottom water on Day 0 cores as well as on Day 10 of the 3 winter treatments

	PO_4^{3-} (µmol l^{-1})		$\frac{dC}{dX}$	Flux
	Bottom water	Peat depth 1.5 cm	(µmol l^{-1} cm^{-1})	(µmol cm^{-2} s^{-1})
Day 0	0.24	7.49	5.18	17×10^{-6}
WinterOX5, Day 10	0.077	1.77	1.21	3.5×10^{-6}
WinterOD5, Day 10	1.25	4.47	2.30	6.7×10^{-6}
WinterOX15, Day 10	1.55	24.4	16.3	68×10^{-6}

for contamination (0.2 µmol l^{-1}) by the microfiber filters determined using Baltic seawater as procedure blanks.

2.8. Total P and Fe in solid samples

After acid digestion using a HNO_3-HF-$HClO_4$ mixture, the contents of total P, Fe and Al in the Day 0 peat sub-samples were analyzed by the same ICP-OES using external calibration and Sc as the internal standard (Dellwig et al. 2019). Precision and trueness for the international reference material SGR-1b (USGS) were better than 5.7 and −5.4 %, respectively.

Since total Fe and P also include refractory Fe and P bound to alumosilicates (here represented by Al), only a portion of total Fe and P in the samples was potentially available for redox reactions. These excess Fe (Fe_{xs}) and P (P_{xs}) fractions were estimated according to the following formula (Dellwig et al. 2007) using Al (8.84 %), Fe (4.83 %) and P (0.07 %) contents of glacial sediments from the Baltic Sea as the lithogenic background (Dellwig et al. 2019):

$$\text{element}_{xs} = \text{element}_{sample} - \text{element}_{glacial\ Baltic} \times \text{Al}_{sample} / \text{Al}_{glacial\ Baltic} \quad (1)$$

2.9. Automated particle analysis

Aliquots were taken from peat sub-samples (depth: 0–0.7 cm) from Day 0 of the winter treatments, resuspended and filtered onto Sartorius Stedim white polycarbonate 25 mm membrane filters (pore size: 0.8 µm). The filters were then dried (21°C, 24 h) and carbon-coated and then underwent automated particle analysis using scanning electron microscopy with energy dispersive X-ray fluorescence (SEM-EDX).

2.10. PolyP quantification

The DAPI-based method of Martin & Van Mooy (2013) was optimized for the extraction and measurement of the polyP-P content in the upper 1 cm layer of each peat sub-sample from the winter treatment obtained on Day 0 and the last day. Due to the rigidity of cyanobacterial cell walls, 7 consecutive freeze–thaw cycles (−20, 24°C) were performed on the sub-samples to cause cell lysis. Further disruption of the cellular material in each sub-sample was carried out by a 10 min bead beating step (glass bead diameter: 0.1 mm; BioSpec Products); sub-samples were subsequently homogenized using a vortex mixer. From each homogenized sub-sample, 200 µg of material was aliquoted and used for measuring polyP-P content. PolyP standards (0, 0.11, 0.22, 0.44, 0.88, 1.75, 3.5 and 7 µmol l^{-1}) were prepared using polyP (mean chain length: 45 ± 5 P) from Sigma-Aldrich (S4379). Both the aliquoted sub-samples and polyP standards underwent DNAse (SKU: 4716728001; Roche) and RNAse (catalog number: AM2288; Invitrogen™) treatment (37°C, 10 min) to minimize matrix effects caused by the binding of DNA and RNA to DAPI. The sub-samples and standards were then incubated with Proteinase K (catalog number: EO0491; Thermo Scientific™) for 10 min at 37°C to digest proteins which could interfere with the DAPI signal. The fluorescence values of the DAPI-treated sub-samples and standards were measured with the TECAN Infinite 200 PRO (fluorescence top precision <2 % CV).

2.11. Microscopic visualization of polyP and filament identification

The presence of a microbial mat and polyP as well as the morphology of polyP-accumulating microorganisms in the surface peat layer were visualized using both light and fluorescence microscopy techniques before the start of the winter, summer and fall treatments. In preparation for fluorescence microscopy, samples were filtered onto a Sartorius Stedim black polycarbonate 25 mm membrane filter (pore size: 0.8 µm) and then stained with 500 µl of DAPI (concentration: 10 mg l^{-1}) for 3 min. The residual DAPI on the filter was then flushed out using Milli-Q water. PolyP forms a complex with DAPI to exhibit a maximum fluorescence emission of 525–550 nm, producing a greenish-yellow hue (Gomes et al. 2013). The DAPI-stained samples were then visualized with a Zeiss Axioskop 2 Mot Plus microscope (360/40 nm excitation). In preparation for light microscopy, a drop of sample (~100 µl) was pipetted onto a glass slide and then enclosed with a 24 × 60 mm coverslip. Light microscopy was then performed with the same microscope, and the generated images were processed using Zeiss ZEN (blue edition) software.

2.12. DNA extraction and 16S rRNA gene sequencing

Two replicates (K1 and K2; 2 ml each) of *in situ* surface peat samples were collected from the same peat fen (approximately 10 cm distance between the re-

plicate collection points), together with the summer treatment cores on Day 0. RNA extraction was performed using the RNeasy PowerSoil Total RNA Kit (Qiagen) following the manufacturer's instructions. The QuantiNova Reverse Transcription Kit (Qiagen) was applied to the RNA sample to yield the final cDNA product. 16S amplicon sequencing was performed on an Illumina MiSeq (2 × 300 bp) by LGC Genomics. The primers used were the modified 341F (5′-CCT AYG GGR BGC ASC AG-3′) and 806R (5′-GGA CTA CNN GGG TAT CTA AT-3′), targeting the V3–V4 regions of the 16S ribosomal DNA (Sundberg et al. 2013).

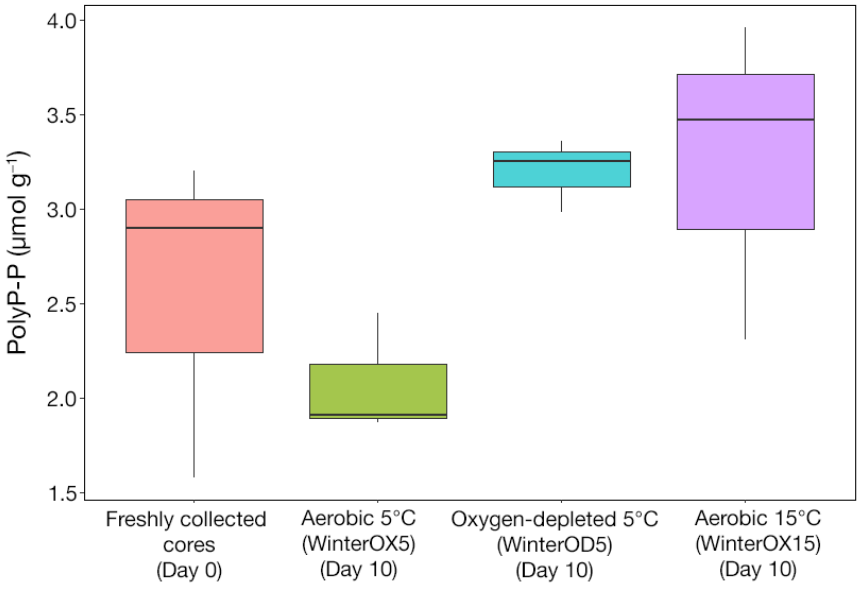

Fig. 3. Boxplot showing the polyP-P content in the upper 1 cm layer of peat in freshly collected cores on Day 0 and in the 3 winter treatments on Day 10. Boxes show upper and lower quartiles; horizontal line: median; whiskers: max./min.

2.13. Sequencing data processing

The obtained primer-clipped forward and reverse reads were joined using QIIME v.1.9.1 (Caporaso et al. 2010) with a minimal overlap of 20 bp. The resulting sequence Multi-Fasta files were processed using the SILVAngs pipeline (SILVAngs v.1.4; Quast et al. 2013), with the pipeline's default settings. Each read was aligned using the SILVA Incremental Aligner (SINA v.1.2.10 for ARB SVN, revision 21008; Pruesse et al. 2012) against the SILVA SSU rRNA SEED. Reads shorter than 50 aligned bases and reads with >2% ambiguities or homopolymers were excluded, as these were likely contaminants and artefacts. Chloroplasts, mitochondria and unknown sequences (0.14 and 0.62% for K1 and K2, respectively) were removed from the 16S analyses. The relative abundance was calculated for each taxon. All obtained sequences have been submitted to the NCBI Sequences Read Archive under Bio Project accession number PRJNA713987.

3. RESULTS

3.1. PolyP accumulation by microorganisms in the peat surface

The mean content of polyP-P in the upper 1 cm layer of the peat in the freshly collected cores (Day 0) of the winter treatment was 2.23 µmol g^{-1} (Fig. 3), comprising 5% of the total P content (49 µmol g^{-1}; Table 3). On Day 10, mean polyP-P content was 2.08, 3.20 and 3.25 µmol g^{-1} in the 3 winter treatments Winter OX5, WinterOD5 and WinterOX15, respectively (Fig. 3). This corresponded to a 0.9× decrease, 1.4× and 1.5× increase in polyP-P, respectively, compared to Day 0. A Wilcoxon rank-sum test was performed to check whether the polyP-P content was significantly different between the

Table 3. Contents of Fe (total and excess [Fe_{xs}]), P (total and excess [P_{xs}]) and Fe:P and Fe_{xs}:P_{xs} molar ratios in 8 surface peat layer replicates during the winter. Fe_{xs} and P_{xs} are the Fe and P fractions potentially available for redox reactions

Replicate	Total Fe (µmol g^{-1})	Fe_{xs} (µmol g^{-1})	Total P (µmol g^{-1})	P_{xs} (µmol g^{-1})	Total Fe: (molar ratio)	Fe_{xs}:P_{xs}P (molar ratio)
1	268	108	44	39	6.0	2.7
2	239	92	38	34	6.3	2.7
3	311	144	53	48	5.9	3.0
4	300	111	49	43	6.1	2.6
5	265	106	43	38	6.1	2.8
6	243	73	43	38	5.6	1.9
7	312	131	57	52	5.4	2.5
8	334	157	61	56	5.5	2.8
Mean	285	115	49	43	5.9	2.6

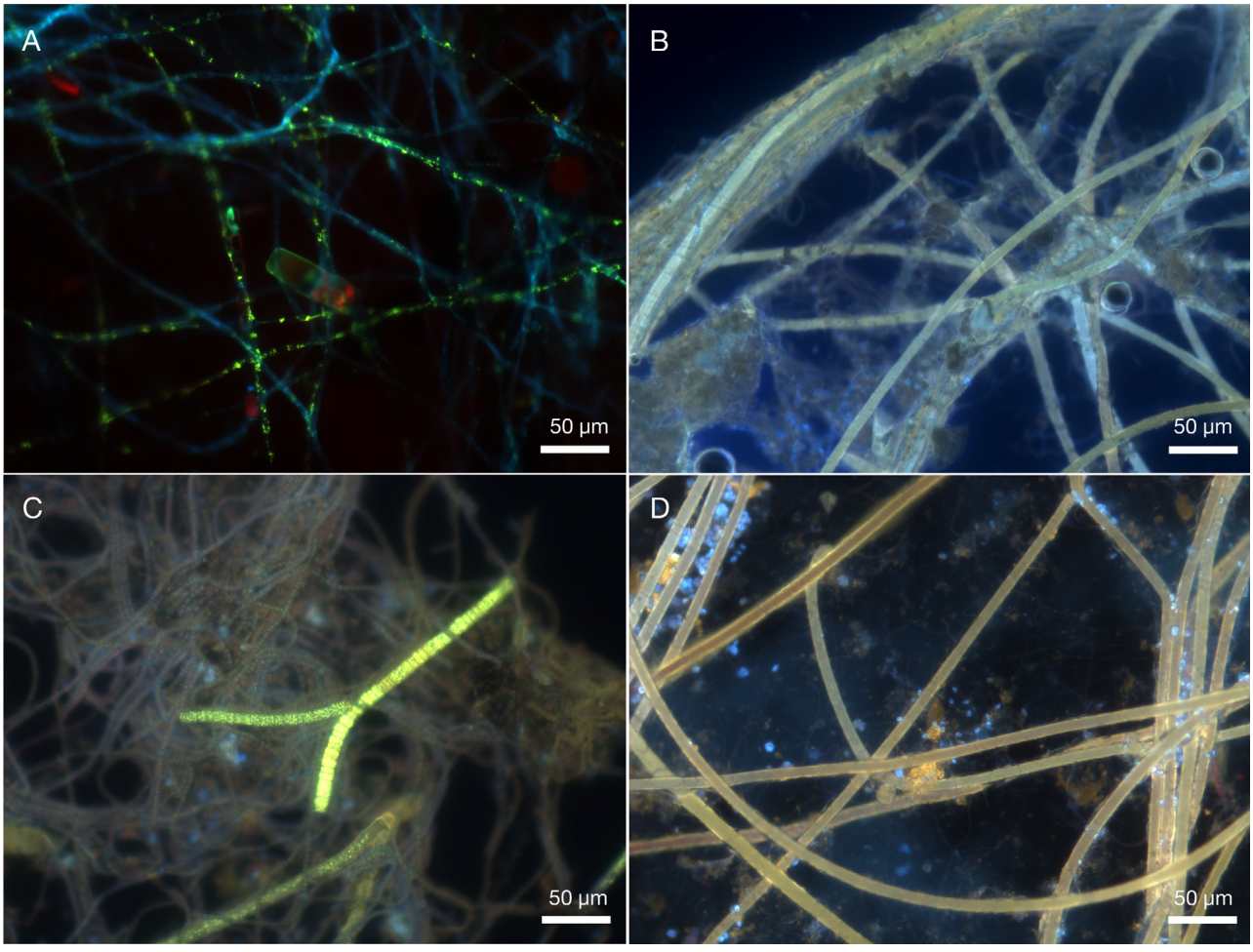

Fig. 4. DAPI-stained fluorescence imaging of the surface peat layer of winter treatment cores on (A) Day 0, and on Day 10 in (B) WinterOX5, (C) WinterOD5 and (D) WinterOX15. A polyP-containing filamentous mat was present in all winter cores as identified by the greenish-yellow fluorescence of polyP at a wavelength of 550 nm. The filaments in WinterOX5 displayed reduced greenish-yellow fluorescence compared to the other 2 winter treatments on Day 10, indicating comparatively lower polyP content in the mat

winter treatments on Day 0 and Day 10. The resulting p-values were 0.66 (WinterOX5), 0.19 (WinterOD5) and 0.38 (WinterOX15), revealing no significant difference ($p \geq 0.05$) in all winter treatments.

Fluorescence microscopy of DAPI-stained samples from Day 0 identified polyP incorporated in filamentous cells, which formed a dense network (Fig. 4A). PolyP inclusions were also observed in diatoms; however, they were extremely sparse compared to the polyP-accumulating filaments (Fig. S1 in the Supplement at www.int-res.com/articles/suppl/m702p019_supp.pdf). When compared to the WinterOD5 and WinterOX15 treatments on Day 10, the filaments of the WinterOX5 treatment revealed a reduced greenish-yellow fluorescence and thus a comparatively lower polyP content (Fig. 4B–D). Filaments similar in morphology to *Lyngbya* spp. on Day 0 also dominated at the end of the WinterOX5 and WinterOX15 incubations (Fig. 4A,B,D). In addition to a significant presence of *Lyngbya*-like filaments (Fig. 4C), thinner polyP-accumulating filaments (mean ± SD diameter: 4.3 ± 0.3 µm) morphologically resembling *Nodularia* spp. (Olenina et al. 2006) were also evident in WinterOD5.

In contrast, polyP-accumulating filaments were missing in the surface peat layer on Days 0 and 10 of the fall treatment FallOD5, but some polyP was present in a few smaller non-filamentous single cells with a diameter range (1–3 µm) comparable to that of typical prokaryotes (Fig. 5).

In addition to some small polyP-accumulating microorganisms, polyP-filled filaments were also clearly identified in the surface peat layer on Day 0 of the SummerOX25 treatment (Fig. 6A). At the end of

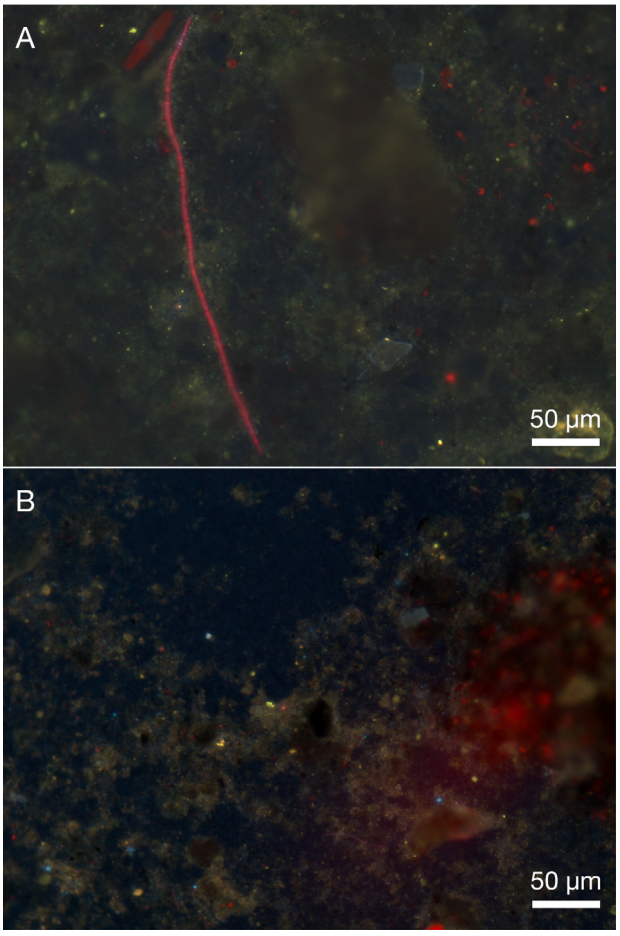

Fig. 5. DAPI-stained fluorescence imaging of the surface peat layer of the FallOD5 treatment on (A) Day 0 and (B) Day 10. While a few smaller cells could be identified, filamentous mats were almost absent in the fall cores

this treatment, which included the removal of the uppermost 1 cm peat layer after Day 2, only the smaller single cells were present (Fig. 6B). Although the surface layer had been removed, samples from the last day of the SummerOD15 (Fig. 6C) and SummerOX15 (Fig. 6D) treatments revealed clumps of mat-forming and polyP-filled filaments with a morphology similar to those on Day 0 as well as a resurgence of the microbial mat. Accompanying light microscopy of the SummerOD15 (Fig. 6E) and SummerOX15 (Fig. 6F) treatment samples also suggested that the filaments belong to unbranched photosynthetic microbes (mean ± SD diameter: 8.9 ± 0.7 µm). Their morphology, length and diameter matched members of the filamentous cyanobacterial order *Oscillatoriales*, which includes polyP-accumulating genera such as *Arthrospira*, *Lyngbya* and *Phormidium* (Sanz-Luque et al. 2020). According to 16S rRNA gene sequencing, filaments of the genus *Lyngbya* were the dominating bacteria in the peat surface layer in summer on Day 0, comprising 27 and 9% of the replicates K1 and K2, respectively (Table S1). The second most abundant cyanobacteria in K1 and K2 belonged to the genera *Nodularia* (0.9% in K1) and *Limnothrix* (0.4% in K2), showing a considerably lower abundance.

3.2. Bulk Fe and P in the surface peat

Mean total Fe and P contents in the peat in winter were 285 and 49 µmol g^{-1}, respectively. The excess contents of both elements added to the less reactive geogenic background were on average 115 µmol g^{-1} for Fe_{xs} and 43 µmol g^{-1} for P_{xs}. The molar Fe_{xs}:P_{xs} ratio among the replicates ranged from 1.9–3.0, with a mean value of 2.6 (Table 3). The good correlation (R^2 = 0.80) between the excess contents suggests Fe oxyhydroxides as a potential source of inorganic P in the peat, though a non-Fe-bound P component is also present as seen in the positive *y*-axis intercept in Fig. S2. SEM-EDX analysis of particles in the surface peat layer showed P content in Fe oxyhydroxides, plagioclase, illite and unidentified organic material (Table S2).

3.3. Bottom water nutrient and Fe trends during incubation

In the winter experiment, PO_4^{3-} concentrations in the bottom water remained low throughout the aerobic, *in situ* temperature treatment WinterOX5 (0.08–0.23 µmol l^{-1}) and even decreased 3× between Days 0 and 10 (Fig. 7A), although polyP-P content also decreased (0.9×) in the same period (Fig. 3, Table 4). In contrast, within the first 2 d of incubation, bottom water PO_4^{3-} increased 6× in the temperature-elevated WinterOX15 and 5× in the oxygen-depleted WinterOD5 treatments and remained at an elevated level until the end of the experiment.

While the FallOD5 treatment was subject to the same conditions as WinterOD5, the abundance of mat-forming filaments was much lower in FallOD5 (Fig. 5). With 2.3 µmol l^{-1} on Day 0, the bottom water PO_4^{3-} concentration was >10× higher in FallOD5 than in WinterOD5 (Fig. 8A). In addition, the PO_4^{3-} concentration in the mat-deficient FallOD5 rapidly reached essentially higher values, with a maximum of 87.4 µmol l^{-1} by Day 10 (Fig. 8A).

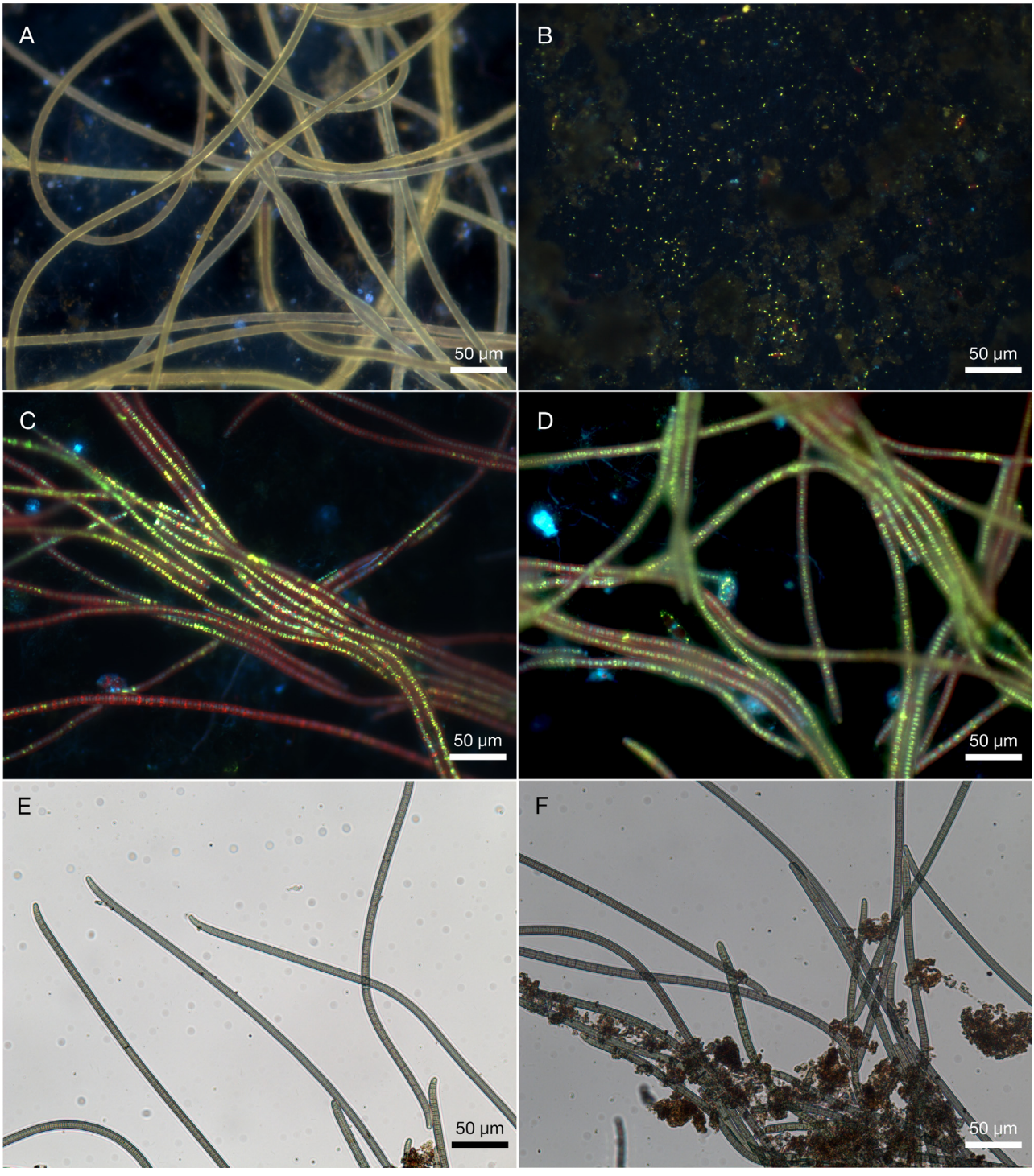

Fig. 6. Microscopic images of the surface peat layers from the summer treatment cores. Fluorescence microscopy showed (A) polyP-filled filaments on Day 0 of the SummerOX25 treatment, (B) absence of filaments but presence of small polyP-accumulating microorganisms in the same treatment at the end of the incubation, and polyP-rich filamentous bacteria in the (C) SummerOD15 and (D) SummerOX15 treatment cores at the end of incubation. (E,F) Light microscopy of photosynthetic filaments from the (E) SummerOD15 and (F) SummerOX15 treatments

In the summer incubation, the PO_4^{3-} concentration in all treatments (SummerOX15, SummerOD15 and SummerOX25) was below 0.5 µmol l^{-1} on Day 0 (Fig. 8C). After removal of the surface peat layer on

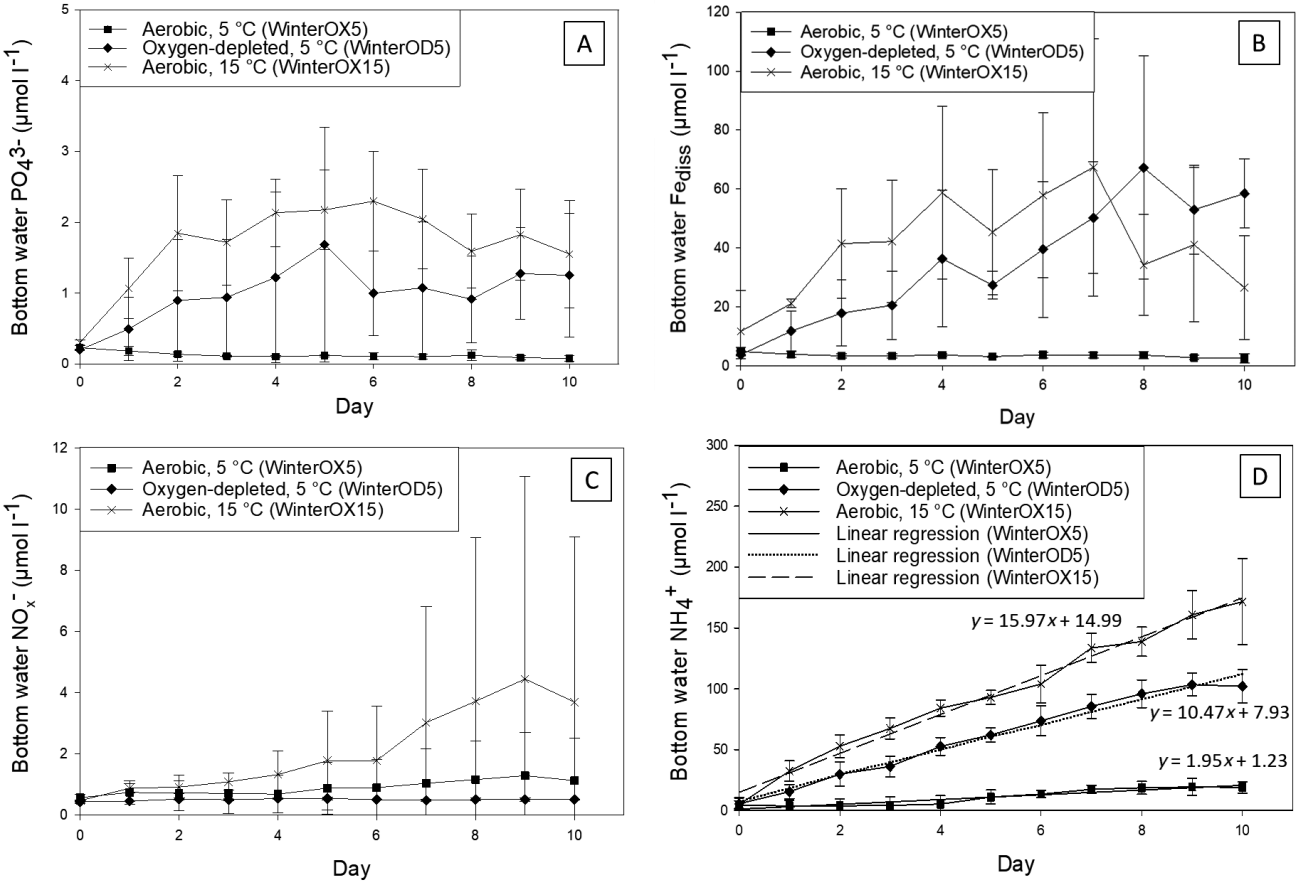

Fig. 7. Bottom water dissolved (A) PO_4^{3-}, (B) dissolved FE (Fe_{diss}), (C) NO_x^- ($NO_3^- + NO_2^-$) and (D) NH_4^+ concentrations (mean ± SD, n = 3) in the 3 winter treatments from Day 0 to Day 10. Linear regression analyses were done on NH_4^+ concentration to estimate the rate of nutrient release from organic matter remineralization in the 3 treatments

Day 2, PO_4^{3-} concentrations strongly increased, especially in SummerOX25 and SummerOD15. After reaching a maximum on Day 4, PO_4^{3-} concentrations decreased rapidly, almost reaching the initial level at Day 8. In contrast, the bottom water PO_4^{3-} in SummerOX15 increased only 1.4× during Days 2–3 and remained nearly constant during Days 3–8.

The bottom water Fe_{diss} concentration in WinterOX5 was low throughout the incubation, and even showed a general decrease during Days 0–10 (1.9×; Fig. 7B). Except for some fluctuations throughout the incubation, the Fe_{diss} concentration in WinterOD5 generally increased during Days 0–10 (16×). In WinterOX15, the bottom water Fe_{diss} concentration had

Table 4. Change in polyP-P content from Day 0 to Day 10 in the upper 1 cm peat layer of the 3 winter treatments, and the equivalent contribution of $\Delta_{polyP\text{-}P}$ to the water column PO_4^{3-} concentration under complete hydrolysis. A hypothetical hydrolysis of the entire polyP pool in the freshly collected peat cores was also calculated to illustrate its corresponding impact on PO_4^{3-} concentration. $\Delta_{polyP\text{-}p}$: change in polyP-P content from Day 0 to Day 10; W_{SL}: mean weight of upper 1 cm of peat layer in core; V_{WC}: mean volume of water column in core; $C_{polyP\text{-}p}$: theoretical change in PO_4^{3-} concentration under total polyP hydrolysis

Treatment	$\Delta_{polyP\text{-}P}$ (µmol g^{-1})	W_{SL} (g)	V_{WC} (ml)	$C_{polyP\text{-}P}$ (µmol l^{-1})
Aerobic, 5°C (WinterOX5)	−0.15	11.2	350	+4.8
Oxygen-depleted, 5°C (WinterOD5)	+1.02	11.2	386	−29.6
Aerobic, 15°C (WinterOX15)	+0.97	11.2	350	−31.0
Hydrolysis of entire polyP content in freshly collected cores (Day 0)	−2.23	11.2	350	+71.4

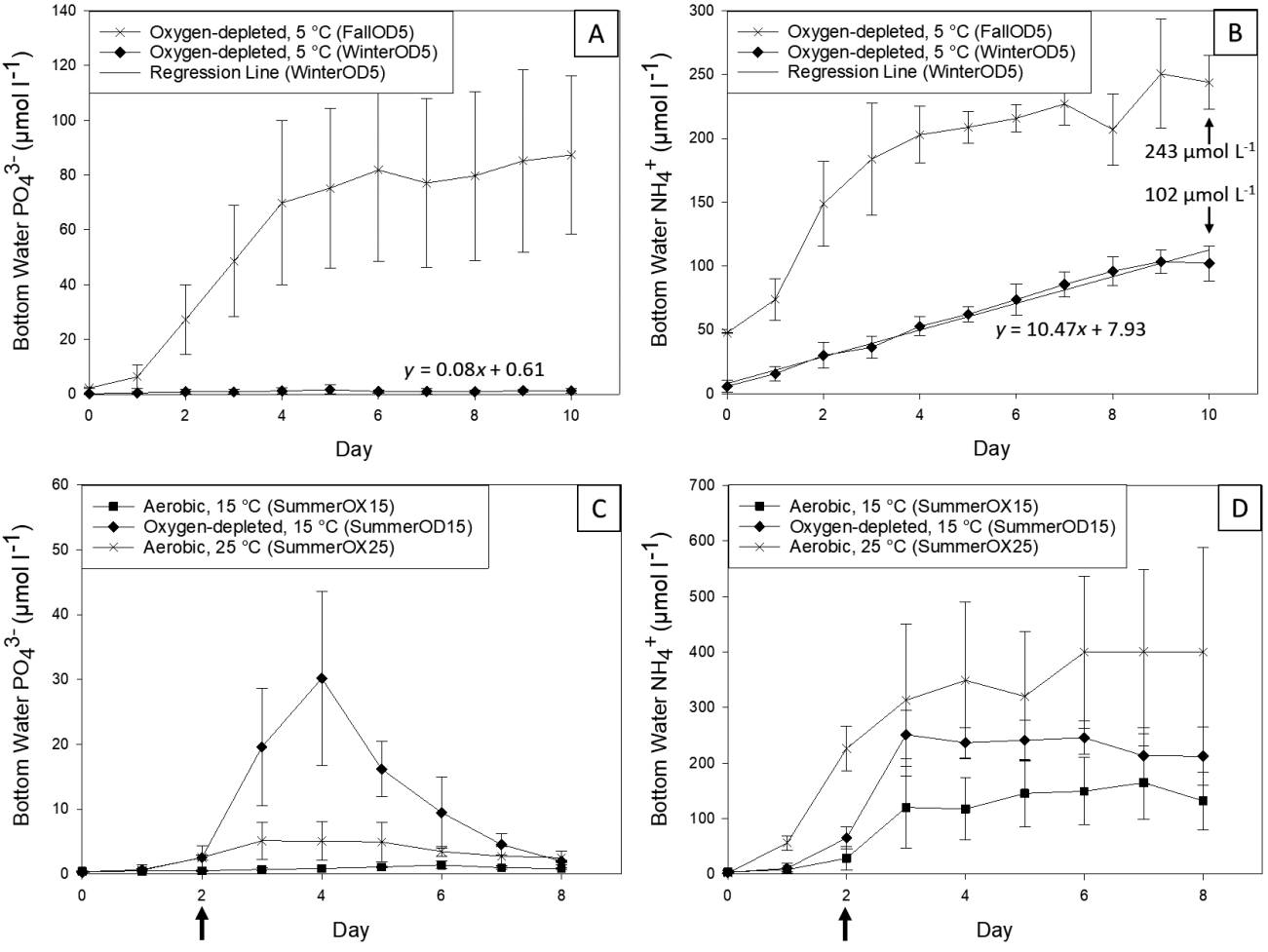

Fig. 8. Concentrations of (A) PO_4^{3-} and (B) NH_4^+ in winter (WinterOD5) and fall (FallOD5) treatments. The PO_4^{3-} concentration was higher in FallOD5 when the mat was nearly absent than in the WinterOD5 treatment where a mat was present. NH_4^+ concentrations were 102 µmol l^{-1} (WinterOD5) and 243 µmol l^{-1} (FallOD5) by Day 10, respectively. Also shown are the (C) PO_4^{3-} and (D) NH_4^+ concentration in the summer treatments throughout the incubation. The concentration of PO_4^{3-} increased most significantly in SummerOD15 after removal of the surface peat layer on Day 2 (indicated by arrows); a sharp decrease of PO_4^{3-} concentration from Day 4 onwards indicated the effect of a PO_4^{3-} uptake mechanism. Data are mean ± SD, n = 3

increased 6× by Day 7 and then decreased 2.5× until the end of the incubation.

While the NO_x^- concentration remained at a low level throughout WinterOD5, increasing concentrations were seen in WinterOX5 and especially Winter OX15 from Day 5 onwards (Fig. 7C). In contrast to the uniform NO_x^- patterns in WinterOX5 and Winter OD5, NO_x^- concentration greatly increased in Winter OX15.

Although the concentration of NH_4^+ increased in WinterOX5 from 4–19 µmol l^{-1}, the overall level remained distinctly lower than in the other winter treatments throughout the entire incubation (Fig. 7D). The level of NH_4^+ gradually increased 18× in WinterOD5 and 35× in WinterOX15. Fig. 9 shows linear regressions for the Day 0–5 and 5–10 segments of the winter treatments, which illustrate the difference in the NH_4^+:PO_4^{3-} increase between both segments and the larger slope for the second segment, respectively.

The NH_4^+ concentration in FallOD5 increased 4× during Days 0–4 and reached 243 µmol l^{-1} at the end of the experiment (Fig. 8B). While the initial NH_4^+ concentration in FallOD5 was 8.4× higher than in WinterOD5, this factor decreased to only 2.4× by Day 10.

After removal of the surface peat layer on Day 2, NH_4^+ concentration increased sharply in both SummerOX15 and SummerOD15 (Fig. 8D). In SummerOX25, however, a sharp rise in NH_4^+ was already

observed before removal of the layer (170× between Days 0 and 3), which was followed by a less pronounced increase until the end of the experiment (1.4×). In contrast, NH_4^+ concentrations were nearly constant in SummerOD15 and SummerOX15 during Days 4–8.

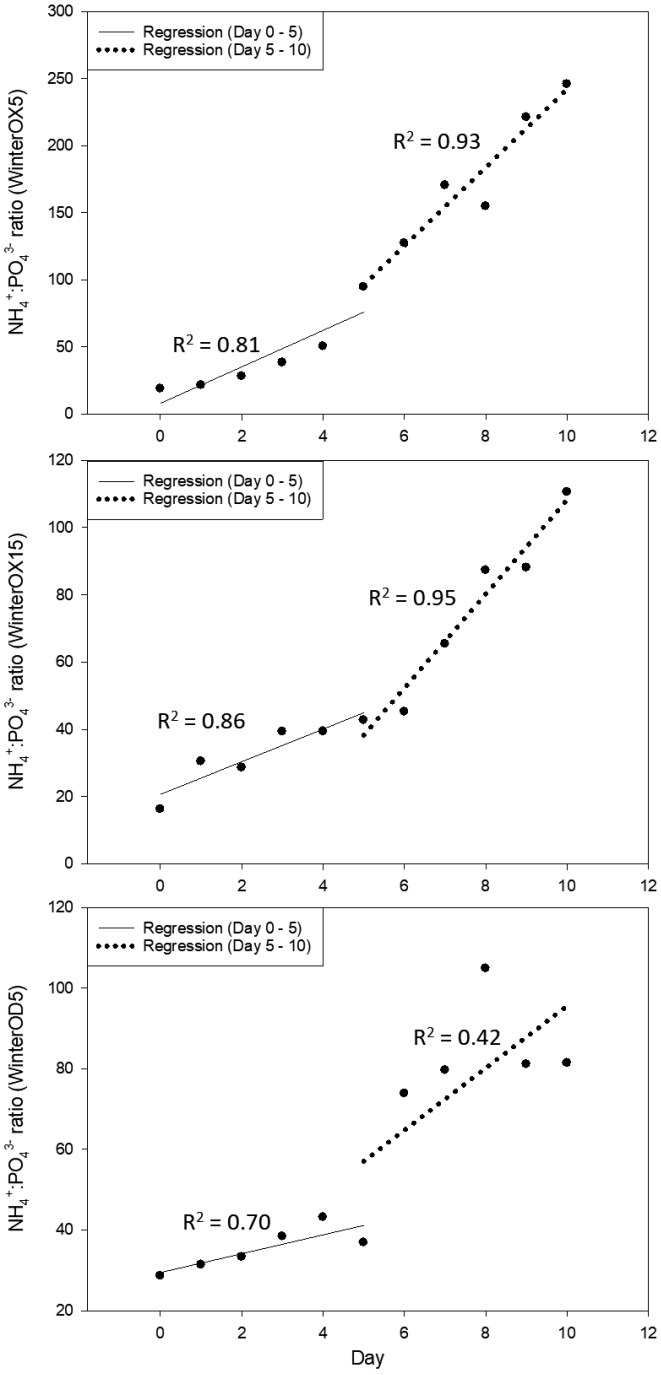

Fig. 9. Comparison of linear-fitted increase between Days 0–5 and 5–10 in the bottom water NH_4^+:PO_4^{3-} ratio of the winter treatment cores

3.4. Dissolved PO_4^{3-} and Fe in bottom water and porewater in winter treatments

Porewater PO_4^{3-} concentration (peat depth: 1.5 cm) was approximately 30× higher than in the overlying bottom water on Day 0 (Fig. 10A, Table 2). On Day 10, porewater PO_4^{3-} concentration at the same peat depth was 23×, 4× and 16× higher than in the bottom water for WinterOX5, WinterOD5 and WinterOX15, respectively. This resulted in a net efflux of PO_4^{3-} from the peat into the water column during all treatments (Table 2). Among the 3 winter treatments on Day 10, PO_4^{3-} flux was highest in WinterOX15 (68×10^{-6} µmol cm^{-2} s^{-1}) and lowest in WinterOX5 (3.5×10^{-6} µmol cm^{-2} s^{-1}).

In contrast to the relatively narrow concentration range of bottom water and porewater Fe_{diss} on Day 0, porewater Fe_{diss} of WinterOX5, WinterOD5 and WinterOX15 at 1.5 cm depth was 26×, 4× and 6× higher than in the bottom water (Fig. 10B).

4. DISCUSSION

4.1. Release and uptake of PO_4^{3-} in winter treatments

The winter incubations subjected to oxygen depletion (WinterOD5) and elevated temperature (WinterOX15) showed both pronounced PO_4^{3-} release to the bottom water (Fig. 7A) and sequestration of polyP by the microbial mat (Figs. 3 & 4), thus strongly contrasting with the relatively stable *in situ* experiments. In the first half of both incubations, the parallel increases in bottom water Fe_{diss} and PO_4^{3-} likely signaled a certain contribution to the bottom water PO_4^{3-} pool via redox-related dissolution of Fe oxyhydroxides and associated P (Fig. 7A,B).

However, the parallel decrease of PO_4^{3-} and Fe_{diss} during the second half of WinterOX15 might also imply that some PO_4^{3-} was trapped by Fe_{diss} precipitating as Fe oxyhydroxides in the peat layer, aside from microbial PO_4^{3-} uptake and polyP accumulation. In the same period, the bottom water PO_4^{3-} concentration in WinterOD5 remained relatively constant, whereas Fe_{diss} further increased (Fig. 7A,B). This might indicate exhaustion of Fe-bound P sources in the peat and a decoupling of Fe and P during the WinterOD5 incubation, as also shown by high porewater Fe_{diss} paralleled by low porewater PO_4^{3-} (Fig. 10) and a lower PO_4^{3-} efflux than in WinterOX15 (Table 2). Furthermore, the discrepancy that the highest porewater Fe_{diss} concentration was in Win-

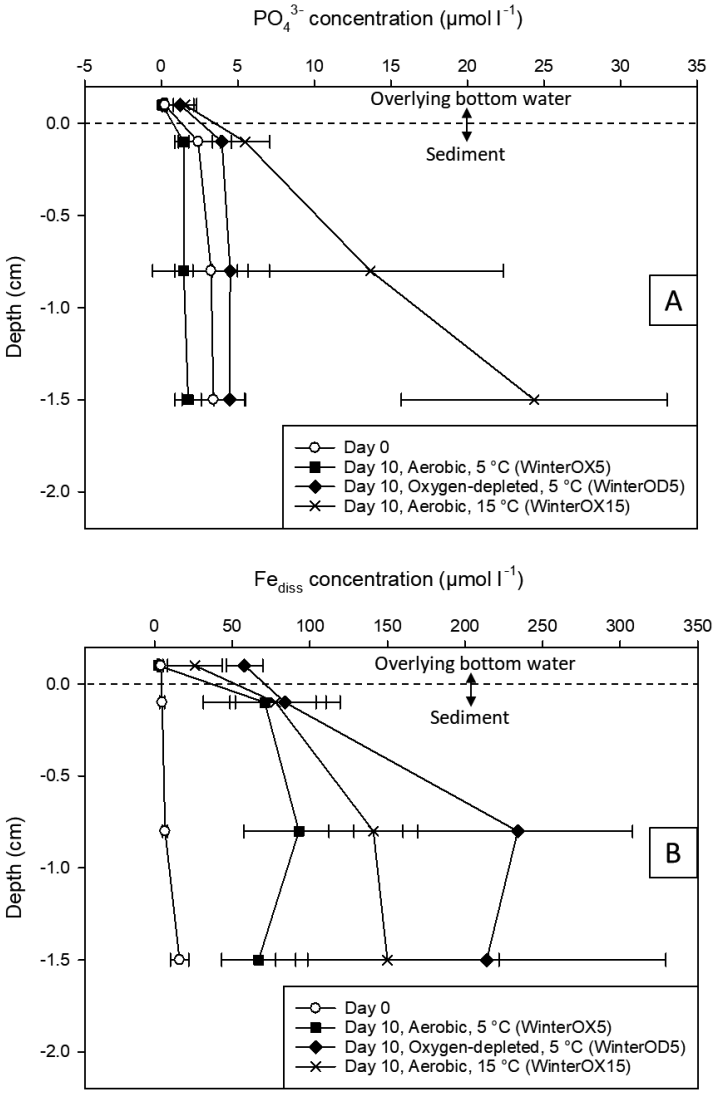

Fig. 10. Concentrations of (A) PO_4^{3-} and (B) dissolved Fe (Fe_{diss}) in the bottom water and porewater (mean ± SD, n = 3) of winter cores on Days 0 and 10 in the WinterOX5, WinterOD5 and WinterOX15 treatments

terOD5 but the highest porewater PO_4^{3-} was instead in WinterOX15 (Fig. 10) suggests that the release of P cannot solely originate from Fe oxyhydroxides.

Furthermore, the relatively low Fe_{xs}:P_{xs} molar ratio of the surface peat samples (mean: 2.6) (Table 3) is comparable to Fe:P ratios of Fe oxyhydroxides and Fe-P mineral phases (Dellwig et al. 2010), which suggests saturation of available P-adsorption sites on the Fe oxyhydroxide compounds present in the peat. This sorption capacity of Fe oxyhydroxides to sequester PO_4^{3-} further declined with increased reducing conditions during the incubation under oxygen-depleted and elevated temperature conditions.

The adsorption of P on sediment particles is also pH-dependent. While P is readily sorbed onto the sediment within a certain pH range (2–8), the amount of adsorbed P decreases rapidly when a threshold at both ends of this range is reached (Zhou et al. 2005). The winter treatments maintained a pH of 6.3–7.5 during the incubation; hence, pH likely had a negligible effect on PO_4^{3-} concentration. Another factor reducing P adsorption onto sediment components (Kleeberg & Kozerski 1997, Perkins & Underwood 2001) is increasing temperature, which increases the molar solubility of compounds at equilibrium within the sediment, thereby reducing P adsorption (Eysseltová et al. 1988). Increasing temperature also augments organic matter degradation and thus internal nutrient cycling and release as well as oxygen consumption (Arnosti et al. 1998). This effect is possibly reflected in the stronger increase of PO_4^{3-} and Fe_{diss} in WinterOX15 than in WinterOD5 (Fig. 7A,B), because the temperature-dependent increase in degradation rate favors both PO_4^{3-} release from organic matter and redox-related dissolution of Fe oxyhydroxides.

Organic matter degradation is the most significant driver of nutrient cycling in sediments, releasing biologically available components like PO_4^{3-} and NH_4^+ (Nixon 1981). Thus, rapidly increasing PO_4^{3-} and NH_4^+ concentrations in both WinterOD5 and WinterOX15 (Fig. 7A,D) indicate that a substantial portion of added PO_4^{3-} originated from this process when considering the stoichiometric coupling of

Table 5. Predicted and actual PO_4^{3-} concentration under elevated temperature conditions (WinterOX15) on Day 10 of the incubation. The temperature coefficient (Q_{10}) varies mostly between 2 and 3 in biological systems and was thus used to approximate 2 different possibilities (Q_{10} = 2, Q_{10} = 3) of PO_4^{3-} concentration in WinterOX15 on Day 10. The PO_4^{3-} concentration of WinterOX15 on Day 0 (0.302 µmol l^{-1}) was used as the *y*-intercept value: (predicted PO_4^{3-} concentration, last day) = (PO_4^{3-} release, 15°C) × (No. of days)

Temperature coefficient (Q_{10})	PO_4^{3-} release, 5°C (µmol l^{-1} d^{-1})	PO_4^{3-} release, 15°C (µmol l^{-1} d^{-1})	PO_4^{3-} concentration, (predicted) 15°C, Day 10 (µmol l^{-1} d^{-1})	PO_4^{3-} concentration, (actual) 15°C, Day 10 (µmol l^{-1})
2	1.95	3.9	39	1.6
3	1.95	5.9	59	1.6

PO_4^{3-} and NH_4^+ release during organic matter degradation (Berner 1977, Krom & Berner 1980).

Nonetheless, a paired *t*-test comparing the bottom water NH_4^+:PO_4^{3-} ratio between the Day 5–10 and 0–5 segments of the winter treatments (Fig. 9) revealed significant p-values less than 0.05 (WinterOX5: 0.0003; WinterOD5: 0.003; WinterOX15: 0.003) and thus an intensified PO_4^{3-} uptake in the second half of the experiment. On the other hand, PO_4^{3-} might also be preferentially released with respect to NH_4^+ during organic matter remineralization under reducing or even sulfidic conditions (Ingall et al. 2005), which could partially explain the low NH_4^+:PO_4^{3-} ratio in the first half of the WinterOD5 incubation. A linear regression fit of the NH_4^+ concentration in *in situ* conditions (WinterOX5) produced a NH_4^+ release rate of 1.95 µmol l^{-1} d^{-1} over the incubation period (Fig. 7D), with the rate of PO_4^{3-} release, in theory, being roughly similar (Paulmier et al. 2009). *In situ* conditions were chosen for this analysis because this minimized any additional NH_4^+ excretion from organisms under temperature-related stress (Whiles et al. 2009). Concurrently, NO_x^- (<5 µmol l^{-1}) concentrations were consistently low (Fig. 7C), suggesting that any loss of NH_4^+ via coupled nitrification–denitrification was only minor. Since the temperature coefficient Q_{10} varies mostly between 2 and 3 in biological systems (Běhrádek 1930, Hochachka 1991), both values were used to approximate the theoretical PO_4^{3-} amount released in the temperature-elevated winter treatment (WinterOX15) at the end of incubation (Table 5). The estimated PO_4^{3-} concentrations were 39 µmol l^{-1} for Q_{10} = 2 and 59 µmol l^{-1} for Q_{10} = 3, which were 24× and 37× higher than the measured PO_4^{3-} concentration of 1.6 µmol l^{-1}. Furthermore, by adding the calculated change in PO_4^{3-} concentration ($C_{polyP\text{-}P}$) in WinterOX15 (Table 4) to the PO_4^{3-} concentration on Day 10, we obtained a value of 33 µmol l^{-1}. This value is 85% of the theoretical PO_4^{3-} concentration for Q_{10} = 2 and 60% for Q_{10} = 3. The high percentages show that the accumulation of polyP between Days 0 and 10 could account for a significant part of the difference between the measured and predicted PO_4^{3-} concentrations at the end of the incubation.

Although the difference in polyP-P content between each winter treatment at Day 10 and the fresh cores collected on Day 0 was not statistically significant ($p > 0.05$), the large $C_{polyP\text{-}P}$ in both WinterOD5 and WinterOX15 showed that polyP accumulation was capable of removing the bulk of PO_4^{3-} from the bottom water (Table 4). Although our results show polyP accumulation under stressed conditions, other studies have revealed inconsistent and organism-specific responses to stressors. For instance, studies using *Escherichia coli* strains showed polyP accumulation (Yoo et al. 2018) but also no effect (Ault-Riché et al. 1998) under heat stress. In wastewater treatment, polyP-accumulating bacteria break down and release polyP under anoxic conditions (Cokro et al. 2017). However, bacteria can also synthesize polyP under reducing conditions and/or absence of light (Shi et al. 2003, Goldhammer et al. 2010).

Overall, the presence of an extensive microbial mat comprising polyP-accumulating filaments in the winter cores, coupled with a significant removal of PO_4^{3-} from the bottom water, indicates that polyP-accumulating organisms can influence the benthic dissolved inorganic P pool, at least at our sampling site. To date, the effect of benthic mat-forming polyP-accumulating organisms on P fluxes is not well-documented. Nevertheless, previous studies have shown a connection between microbial mats and sedimentary P retention. The concentration of soluble reactive phosphorus in streams was negatively correlated with the polyP: total periphyton P ratio, and P spikes during storms stimulated polyP accumulation by mat-like periphyton (Rier et al. 2016). On geologic time scales, fossilized microbial mats found in phosphate-rich layers (Williams & Reimers 1983, Reimers et al. 1990, Bailey et al. 2007, Diaz et al. 2008) suggest that mat-forming bacteria were engaged in phosphogenesis. In addition, the dissolution of microbial polyP can contribute directly to apatite precipitation, and subsequently the deposition of phosphorites as a long-term P sink in the Namibian shelf (Goldhammer et al. 2010). The microbial polyP pool is increasingly being recognized as a key component of the P cycle in marine sediments. In an empirical diagenetic model of anoxic shelf sediments, P burial was approximately 30% lower in sediments without a polyP-driven microbial P pump compared to the baseline model (Dale et al. 2016). The modified model integrated microbial-synthesized polyP as an intermediate, which could be consequently converted to either unreactive particulate or bulk organic P such as phosphate esters and phosphonates. Although this diagenetic model covers processes over a long time scale, the outcome suggests that microbial polyP in the sediment is crucial to P sequestration. Although polyP comprised only ~5% of the total P pool in the upper 1 cm peat layer in our *in situ*

treatment, its complete hydrolysis would result in a $C_{polyP\text{-}P}$ (+71.4 µmol l^{-1}; Table 4) which is 260× higher than the bottom water PO_4^{3-} concentration on Day 0 (0.3 µmol l^{-1}; Fig. 7A). Furthermore, this percentage increases when deducting e.g. refractory P components less involved in active nutrient cycling; therefore, the influence of polyP in benthic P cycling should not be disregarded. And since microbes are capable of accumulating polyP at large intracellular levels (Sanz-Luque et al. 2020), polyP-accumulating bacterial mats deserve more attention in future studies.

4.2. Relationship between PO_4^{3-} uptake and microbial mats

Fluorescence microscopy (Fig. 6A) closely reflected the dominance of *Lyngbya* spp. (Table S1) in the surface peat layer on Day 0 of the summer experiment. No 16S rRNA amplicon sequencing was available for the end of the summer treatments or the winter and fall treatments; however, both light and fluorescence microscopy provided insights into the microbial community to a certain extent. When comparing the SummerOX15 (Fig. 6B) and Summer OX5/SummerOD5 (Fig. 6C,D) samples with the Day 0 (Fig. 6A) samples, the microbial community in SummerOX15 appeared more distinct due to the dominance of small polyP-accumulating bacteria over *Lyngbya*-like filaments. The dominance of *Lyngbya*- and *Nodularia*-like filaments in the winter treatments (Fig. 4) also matched the relative abundance profile shown in Table S1. On the contrary, the near absence of filamentous bacteria in FallOD5 (Fig. 5) reflected a microbial community structure which was obviously different from the winter and summer treatments. It is therefore likely that polyP-accumulating members of the microbial community in the surface peat layer change according to varying environmental conditions.

The potential PO_4^{3-} retention caused by the *Lyngbya*-dominated bacterial mat was underpinned by contrasting the oxygen-depleted winter and fall treatments, with the latter showing essentially higher concentrations and release rates of PO_4^{3-} in the absence of a mat (Fig. 8A), while the difference in NH_4^+ concentration between the 2 treatments was comparatively smaller (Fig. 8B). A linear regression also showed the release rate of NH_4^+ in WinterOD5 to be 10.5 µmol l^{-1} d^{-1} (Fig. 8B), which was 130× higher than the rate of PO_4^{3-} release (0.08 µmol l^{-1} d^{-1}; Fig. 8A) over the course of the incubation. The theoretical sequestration of PO_4^{3-} from the bottom water calculated from the increased polyP-P content in WinterOD5 (Table 4) also supports this assumption. Thus, a scenario is probable in which a polyP-accumulating microbial mat mitigates a PO_4^{3-} upsurge, as polyP can comprise >40% of the non-reactive P pool in surface lake sediments while declining to less than 10% just 1 cm below the surface (Hupfer et al. 2004). Given the huge disparity in PO_4^{3-} concentration between the treatments, the constant removal, sequestration and burial of significant amounts of dissolved inorganic P over a long time (Crosby & Bailey 2012) could potentially be considered a precursor for phosphogenesis along the coastal wetlands of the southern Baltic Sea. On the other hand, the composition of organic matter and P fractions in the peat in WinterOD5 and FallOD5 were not analyzed. It is possible that differences in peat composition due to, e.g. local patchiness and seasonality existed between the FallOD5 and WinterOD5 treatments, contributing to different rates of PO_4^{3-} release. However, we perceived these differences to be minor due to the relative physical stability of our sampling site, which is only irregularly flooded during storms in winter and fall.

In the summer treatments, the removal of the surface peat layer also highlighted the role of the microbial mat in mitigating increasing bottom water PO_4^{3-} levels (Fig. 8C,D), especially in SummerOD15. The removal of the surface peat layer including the mat on Day 2 likely reduced the number of active PO_4^{3-} sorption sites and exposed porewaters below, initially resulting in an increased PO_4^{3-} efflux (Fig. 8C). However, the subsequent sharp decrease in PO_4^{3-} concentration signaled a loss of PO_4^{3-} from the water column, which was at least to some extent due to polyP accumulation by the re-establishing *Lyngbya*-dominated mat (Fig. 6C) (Ahern et al. 2007). The concurrent occurrence of both PO_4^{3-} loss and mat re-establishment suggests the conversion of a large amount of PO_4^{3-} into biogenic polyP. A high NH_4^+ concentration in the summer treatment cores also likely allowed for adequate microbial N assimilation, which would have driven microbial growth. At the end of the SummerOD15 incubation, the PO_4^{3-} concentration was at a level similar to that before the removal of the surface layer. Since this treatment was oxygen-depleted, redox-sensitive compounds in the peat most likely had a limited sorption capacity for the removal of dissolved PO_4^{3-}. And although aerobic conditions are the most ideal for organic matter degradation, oxygen depletion would still have driven the anaerobic decomposition of organic matter, lead-

ing to the release of PO_4^{3-} from organic P fractions (Holmer 1999, Bastviken et al. 2004). In SummerOX25, the dominance of tiny polyP-accumulating bacteria instead of larger filamentous bacteria at the end of the incubation (Fig. 6A,B) could mean that smaller polyP-storing microorganisms might have a distinct impact on PO_4^{3-} removal if present in sufficient quantity. In contrast to NH_4^+, PO_4^{3-} release was much lower in SummerOX25 from Days 0–3 (Fig. 8C,D), indicating possible retention of PO_4^{3-} in the surface layer. Similar to WinterOX15, the decrease in PO_4^{3-} in the SummerOX25 treatment from Days 3–8 was accompanied by an ongoing increase in NH_4^+ (Figs. 7A,D & 8C,D), which implied a net PO_4^{3-} efflux from the water column into the peat. Nevertheless, in order to determine the extent to which polyP-accumulating organisms regulate PO_4^{3-} fluxes at the peat–water interface, more data on the quantity of microbial polyP accumulation and the different P fractions in the peat are needed. With such additional data available, it would be possible to construct a mass-balance P budget to relate the amount of accumulated polyP to the total PO_4^{3-} removed from the bottom water. The habitat at our study site was patchy and likely contained various P pools as revealed by SEM-EDX analysis (Table S2), hence it was not possible to track each P pool precisely over time. These P-containing compounds would therefore comprise the remaining 95% of P in addition to polyP in the surface peat layer. Previous studies have also highlighted the contribution of polyP metabolism to the benthic P flux by showing that polyP comprises a significant amount of the total P in the sediment and that P release from the breakdown of microbial polyP might explain part of the P flux under anoxic conditions (Sannigrahi & Ingall 2005, Hupfer & Lewandowski 2008). However, to the best of our knowledge, there is still no successful record of a mass-balance budget linking sediment polyP metabolism to the dissolved inorganic P pool in the overlying water column. Across different environments, organic P and redox-dependent compounds such as Fe- and Mn-bound P fractions in the sediment constitute a part of the P cycle to varying degrees. Sediments might also contain significant amounts of redox-stable P-binding components such as bauxites and unreducible Fe minerals such as ilmenite, which are capable of influencing P release via P retention (Von Gruenewaldt 1993, Hupfer & Lewandowski 2008). By quantifying these various P sources, the significance of the microbial polyP role in the benthic P flux can be more precisely determined.

5. CONCLUSIONS

There is growing evidence of a significant biological role in P cycling at the sediment–water interface which should be given more recognition. Circumstantial evidence from laboratory experiments in this study showed that a microbial mat community dominated by filaments of the genus *Lyngbya* contributed to a mediation of P cycling in the short term. Under varying conditions of elevated temperature and oxygen depletion, an increase in bottom water PO_4^{3-} concentrations from PO_4^{3-} release mechanisms such as organic matter remineralization and Fe-bound P dissolution was counteracted through PO_4^{3-} uptake by mat-forming polyP-accumulating organisms in the surface peat layer. The presence of a mat of polyP-accumulating microorganisms (after surface layer removal on Day 2) at the end of a summer incubation implied that a portion of bottom water PO_4^{3-} was removed and stored as polyP in the surface peat. The markedly reduced presence of such a mat in the negative control treatment in fall essentially resulted in a much higher bottom water PO_4^{3-} level at the end of the incubation. Changes in PO_4^{3-} concentration could thus be explained by this biological component, and studies should be carried out at other sites to determine whether this is a general feature in coastal peatlands. Although comprising only ~5% of the total P pool in the peat, polyP is potentially a crucial component within the P cycle, being able to significantly impact water column PO_4^{3-} levels at least on short time scales. The role of the benthic microbial layer in P cycling should be taken more into account and could represent an essential step in mitigating spikes in dissolved P levels in aquatic ecosystems.

Data availability. Data regarding the 16S rRNA gene sequences from the surface peat samples collected from Karrendorfer Wiesen can be accessed via the NCBI Read Archive at https://dataview.ncbi.nlm.nih.gov/object/PRJNA713987?reviewer=vjsac25lkvcoc38ndo5s6uesqu. Other data associated with the figures in this article can be accessed in the EarthChem library at https://doi.org/10.26022/IEDA/112070.

Acknowledgements. We thank the working group Geomicrobiology at the Leibniz Institute for Baltic Sea Research (IOW) for their ideas and guidance. We are also grateful to Christian Burmeister for running the nutrient analyses, Anne Köhler for supporting ICP analytics, Sascha Plewe for performing the SEM-EDX analyses and Christin Laudan for assisting with setting up the incubation experiments. Special thanks also to Philipp Braun for instruction on the polyP-P measurement method, Brittan Scales and Munyaradzi Tambo for their guidance in preparing the samples for 16S rRNA gene sequencing and the IOW workshop for designing and building sampling equipment. We also

express our gratitude to the handling editor and the 3 reviewers for the evaluation of this work. This study was funded by the Deutsche Forschungsgemeinschaft (DFG) under grant number GRK 2000.

LITERATURE CITED

Achbergerová L, Nahálka J (2011) Polyphosphate — an ancient energy source and active metabolic regulator. Microb Cell Fact 10:63

Ahern KS, Ahern CR, Savige GM, Udy JW (2007) Mapping the distribution, biomass and tissue nutrient levels of a marine benthic cyanobacteria bloom (*Lyngbya majuscula*). Mar Freshw Res 58:883–904

Arnosti C, Jørgensen BB, Sagemann J, Thamdrup B (1998) Temperature dependence of microbial degradation of organic matter in marine sediments: polysaccharide hydrolysis, oxygen consumption, and sulfate reduction. Mar Ecol Prog Ser 165:59–70

Arthur KE, Paul VJ, Paerl HW, O'Neil JM, Joyner J, Meickle T (2009) Effects of nutrient enrichment of the cyanobacterium *Lyngbya* sp. on growth, secondary metabolite concentration and feeding by the specialist grazer *Stylocheilus striatus.* Mar Ecol Prog Ser 394:101–110

Ault-Riché D, Fraley CD, Tzeng CM, Kornberg A (1998) Novel assay reveals multiple pathways regulating stress-induced accumulations of inorganic polyphosphate in *Escherichia coli.* J Bacteriol 180:1841–1847

Bailey JV, Joye SB, Kalanetra KM, Flood BE, Corsetti FA (2007) Evidence of giant sulphur bacteria in Neoproterozoic phosphorites. Nature 445:198–201

Bastviken D, Persson L, Odham G, Tranvik L (2004) Degradation of dissolved organic matter in oxic and anoxic lake water. Limnol Oceanogr 49:109–116

Běhrádek J (1930) Temperature coefficients in biology. Biol Rev Camb Philos Soc 5:30–58

Berg P, Risgaard-Petersen N, Rysgaard S (1998) Interpretation of measured concentration profiles in sediment pore water. Limnol Oceanogr 43:1500–1510

Berner RA (1977) Stoichiometric models for nutrient regeneration in anoxic sediments. Limnol Oceanogr 22:781–786

Bernhardt KG, Koch M (2003) Restoration of a salt marsh system: temporal change of plant species diversity and composition. Basic Appl Ecol 4:441–451

Boudreau BP (1997) Diagenetic models and their implementation: modelling transport and reactions in aquatic sediments, 1st edn. Springer, Berlin

Brock J, Schulz-Vogt HN (2011) Sulfide induces phosphate release from polyphosphate in cultures of a marine *Beggiatoa* strain. ISME J 5:497–506

Caporaso JG, Kuczynski J, Stombaugh J, Bittinger K and others (2010) QIIME allows analysis of high-throughput community sequencing data. Nat Methods 7:335–336

Carstensen J, Conley DJ, Almroth-Rosell E, Asmala E and others (2020) Factors regulating the coastal nutrient filter in the Baltic Sea. Ambio 49:1194–1210

Cokro AA, Law Y, Williams RBH, Cao Y, Nielsen PH, Wuertz S (2017) Non-denitrifying polyphosphate accumulating organisms obviate requirement for anaerobic condition. Water Res 111:393–403

Comeau Y, Hall K, Hancock R, Oldham W (1986) Biochemical model for enhanced biological phosphorus removal. Water Res 20:1511–1521

Crosby CH, Bailey JV (2012) The role of microbes in the formation of modern and ancient phosphatic mineral deposits. Front Microbiol 3:241

Dale AW, Boyle RA, Lenton TM, Ingall ED, Wallmann K (2016) A model for microbial phosphorus cycling in bioturbated marine sediments: significance for phosphorus burial in the early Paleozoic. Geochim Cosmochim Acta 189:251–268

Dellwig O, Bosselmann K, Kölsch S, Hentscher M and others (2007) Sources and fate of manganese in a tidal basin of the German Wadden Sea. J Sea Res 57:1–18

Dellwig O, Leipe T, März C, Glockzin M and others (2010) A new particulate Mn–Fe–P-shuttle at the redoxcline of anoxic basins. Geochim Cosmochim Acta 74:7100–7115

Dellwig O, Wegwerth A, Schnetger B, Schulz H, Arz HW (2019) Dissimilar behaviors of the geochemical twins W and Mo in hypoxic–euxinic marine basins. Earth Sci Rev 193:1–23

Diaz J, Ingall E, Benitez-Nelson C, Paterson D, de Jonge MD, McNulty I, Brandes JA (2008) Marine polyphosphate: a key player in geologic phosphorus sequestration. Science 320:652–655

Eysseltová J, Dirkse TP, Makovička J, Salomon M (eds) (1988) Alkali metal orthophosphates. Solubility data series, Vol 31. Pergamom Press, New York, NY

Flemming BW, Delafontaine MT (2000) Mass physical properties of muddy intertidal sediments: some applications, misapplications and non-applications. Cont Shelf Res 20: 1179–1197

Gächter R, Meyer JS (1993) The role of microorganisms in mobilization and fixation of phosphorus in sediments. Hydrobiologia 253:103–121

Goldhammer T, Brüchert V, Ferdelman TG, Zabel M (2010) Microbial sequestration of phosphorus in anoxic upwelling sediments. Nat Geosci 3:557–561

Gomes FM, Ramos IB, Wendt C, Girard-Dias W, de Souza W, Machado EA, Miranda K (2013) New insights into the *in situ* microscopic visualization and quantification of inorganic polyphosphate stores by 4′,6-diamidino-2-phenylindole (DAPI)-staining. Eur J Histochem 57:e34

Hansen HP, Koroleff F (1999) Determination of nutrients. In: Grasshoff K, Kremling K, Ehrhardt M (eds) Methods of seawater analysis, 3rd edn. Wiley-VCH Verlag, Weinheim, p 159–228

Hermans M, Lenstra WK, van Helmond NAGM, Behrends T and others (2019) Impact of natural re-oxygenation on the sediment dynamics of manganese, iron and phosphorus in a euxinic Baltic Sea basin. Geochim Cosmochim Acta 246:174–196

Hochachka PW (1991) Temperature: the ectothermy option. In: Hochachka PW, Mommsen TP (eds) Biochemistry and molecular biology of fishes, Vol 1. Elsevier Science Publishers, Amsterdam, p 313–322

Holmer M (1999) The effect of oxygen depletion on anaerobic organic matter degradation in marine sediments. Estuar Coast Shelf Sci 48:383–390

Hupfer M, Lewandowski J (2008) Oxygen controls the phosphorus release from lake sediments — a long-lasting paradigm in limnology. Int Rev Hydrobiol 93:415–432

Hupfer M, Rübe B, Schmieder P (2004) Origin and diagenesis of polyphosphate in lake sediments: a ^{31}P-NMR study. Limnol Oceanogr 49:1–10

Ingall ED, Jahnke R (1997) Influence of water-column anoxia on the elemental fractionation of carbon and phosphorus during sediment diagenesis. Mar Geol 139:219–229

Ingall ED, Kolowith L, Lyons T, Hurtgen M (2005) Sediment carbon, nitrogen and phosphorus cycling in an anoxic fjord, Effingham Inlet, British Columbia. Am J Sci 305: 240–258

Jensen HS, Thamdrup B (1993) Iron-bound phosphorus in marine sediments as measured by bicarbonate-dithionite extraction. Hydrobiologia 253:47–59

Jørgensen C, Jensen HS, Andersen FØ, Egemose S, Reitzel K (2011) Occurrence of orthophosphate monoesters in lake sediments: significance of *myo*- and *scyllo*-inositol hexakisphosphate. J Environ Monit 13:2328–2334

Kerrn-Jespersen JP, Henze M (1993) Biological phosphorus uptake under anoxic and aerobic conditions. Water Res 27:617–624

Kleeberg A, Kozerski HP (1997) Phosphorus release in Lake Großer Müggelsee and its implications for lake restoration. In: Kufel L, Prejs A, Rybak JI (eds) Shallow lakes '95. Developments in hydrobiology, Vol 119. Springer, Dordrecht, p 9–26

Kornberg A, Rao NN, Ault-Riché D (1999) Inorganic polyphosphate: a molecule of many functions. Annu Rev Biochem 68:89–125

Krause J, Hopwood MJ, Höfer J, Krisch S and others (2021) Trace element (Fe, Co, Ni and Cu) dynamics across the salinity gradient in Arctic and Antarctic glacier fjords. Front Earth Sci 9:725279

Krom MD, Berner RA (1980) The diffusion coefficients of sulfate, ammonium, and phosphate ions in anoxic marine sediments. Limnol Oceanogr 25:327–337

Lake BA, Coolidge KM, Norton SA, Amirbahman A (2007) Factors contributing to the internal loading of phosphorus from anoxic sediments in six Maine, USA, lakes. Sci Total Environ 373:534–541

Langer S, Vogts A, Schulz-Vogt HN (2018) Simultaneous visualization of enzymatic activity in the cytoplasm and at polyphosphate inclusions in *Beggiatoa* sp. strain 35Flor incubated with ^{18}O-labeled water. MSphere 3:e00489-18

Li J, Plouchart D, Zastepa A, Dittrich M (2019) Picoplankton accumulate and recycle polyphosphate to support high primary productivity in coastal Lake Ontario. Sci Rep 9:19563

Lundin L, Nilsson T, Jordan S, Lode E, Strömgren M (2017) Impacts of rewetting on peat, hydrology and water chemical composition over 15 years in two finished peat extraction areas in Sweden. Wetlands Ecol Manage 25:405–419

Martin P, Van Mooy BA (2013) Fluorometric quantification of polyphosphate in environmental plankton samples: extraction protocols, matrix effects, and nucleic acid interference. Appl Environ Microbiol 79:273–281

McColl RHS (1977) Chemistry of sediments in relation to trophic condition of eight Rotorua Lakes. NZ J Mar Freshw Res 11:509–523

McMahon KD, Read EK (2013) Microbial contributions to phosphorus cycling in eutrophic lakes and wastewater. Annu Rev Microbiol 67:199–219

Mortimer CH (1942) The exchange of dissolved substances between mud and water in lakes. J Ecol 30:147–201

Nixon SW (1981) Remineralization and nutrient cycling in coastal marine ecosystems. In: Neilson BJ, Cronin LE (eds) Estuaries and nutrients. Contemporary issues in science and society. Humana Press, Clifton, NJ, p 111–138

Nocek B, Kochinyan S, Proudfoot M, Brown G and others (2008) Polyphosphate-dependent synthesis of ATP and ADP by the family-2 polyphosphate kinases in bacteria. Proc Natl Acad Sci USA 105:17730–17735

Olenina I, Hajdu S, Andersson A, Edler L and others (2006) Biovolumes and size-classes of phytoplankton in the Baltic Sea. Balt Sea Environmental Proceedings No. 106. HELCOM Baltic Marine Environment Protection Commission, Helsinki

Paulmier A, Kriest I, Oschlies A (2009) Stoichiometries of remineralisation and denitrification in global biogeochemical ocean models. Biogeosciences 6:923–935

Perkins RG, Underwood GJC (2001) The potential for phosphorus release across the sediment–water interface in an eutrophic reservoir dosed with ferric sulphate. Water Res 35:1399–1406

Pruesse E, Peplies J, Glöckner FO (2012) SINA: accurate high-throughput multiple sequence alignment of ribosomal RNA genes. Bioinformatics 28:1823–1829

Quast C, Pruesse E, Yilmaz P, Gerken J and others (2013) The SILVA ribosomal RNA gene database project: improved data processing and web-based tools. Nucleic Acids Res 41:D590–D596

Rao NN, Gómez-García MR, Kornberg A (2009) Inorganic polyphosphate: Essential for growth and survival. Annu Rev Biochem 78:605–647

Reimers CE, Kastner M, Garrison RE (1990) The role of bacterial mats in phosphate mineralization with particular reference to the Monterey Formation. In: Riggs SR, Burnett WC (eds) Phosphate deposits of the world, Vol 3: genesis of neogene to modern phosphorites. Cambridge University Press, Cambridge, p 301–311

Rier ST, Kinek KC, Hay SE, Francoeur SN (2016) Polyphosphate plays a vital role in the phosphorus dynamics of stream periphyton. Freshw Sci 35:490–502

Rivas-Lamelo S, Benzerara K, Lefèvre CT, Monteil CL and others (2017) Magnetotactic bacteria as a new model for P sequestration in the ferruginous Lake Pavin. Geochem Perspect Lett 5:35–41

Rubio-Rincón FJ, Welles L, Lopez-Vazquez CM, Nierychlo M and others (2017) Long-term effects of sulphide on the enhanced biological removal of phosphorus: the symbiotic role of *Thiothrix caldifontis.* Water Res 116:53–64

Sannigrahi P, Ingall E (2005) Polyphosphates as a source of enhanced P fluxes in marine sediments overlain by anoxic waters: evidence from ^{31}P NMR. Geochem Trans 6:52

Sanz-Luque E, Bhaya D, Grossman AR (2020) Polyphosphate: a multifunctional metabolite in cyanobacteria and algae. Front Plant Sci 11:938

Schulz HN, Schulz HD (2005) Large sulfur bacteria and the formation of phosphorite. Science 307:416–418

Schulz HD, Zabel M (eds) (2006) Marine geochemistry, 1st edn. Springer-Verlag, Berlin/Heidelberg

Schulz-Vogt HN, Pollehne F, Jürgens K, Arz HW and others (2019) Effect of large magnetotactic bacteria with polyphosphate inclusions on the phosphate profile of the suboxic zone in the Black Sea. ISME J 13:1198–1208

Seeberg-Elverfeldt J, Schlüter M, Feseker T, Kölling M (2005) Rhizon sampling of porewaters near the sediment–water interface of aquatic systems. Limnol Oceanogr Methods 3:361–371

Seiberling S, Stock M (2009) Renaturierung von Salzgrasländern bzw. Salzwiesen der Küsten. In: Zerbe S, Wiegleb G (eds) Renaturierung von Ökosystemen in Mitteleuropa. Spektrum Akademischer Verlag, Heidelberg, p 183–209

Shi X, Yang L, Niu X, Xiao L, Kong Z, Qin B, Gao G (2003) Intracellular phosphorus metabolism of *Microcystis aeruginosa* under various redox potential in darkness. Microbiol Res 158:345–352

Sundberg C, Al-Soud WA, Larsson M, Alm E and others (2013) 454 pyrosequencing analyses of bacterial and archaeal richness in 21 full-scale biogas digesters. FEMS Microbiol Ecol 85:612–626

Viktorsson L, Ekeroth N, Nilsson M, Kononets M, Hall POJ (2013) Phosphorus recycling in sediments of the central Baltic Sea. Biogeosciences 10:3901–3916

Von Gruenewaldt G (1993) Ilmenite–apatite enrichments in the upper zone of the Bushveld Complex: a major titanium-rock phosphate resource. Int Geol Rev 35:987–1000

Weil M, Wang H, Bengtsson M, Köhn D and others (2020) Long-term rewetting of three formerly drained peatlands drives congruent compositional changes in pro- and eukaryotic soil microbiomes through environmental filtering. Microorganisms 8:550

Whiles MR, Huryn AD, Taylor BW, Reeve JD (2009) Influence of handling stress and fasting on estimates of ammonium excretion by tadpoles and fish: recommendations for designing excretion experiments. Limnol Oceanogr Methods 7:1–7

Williams LA, Reimers C (1983) Role of bacterial mats in oxygen-deficient marine basins and coastal upwelling regimes: preliminary report. Geology 11:267–269

Xie L, Jakob U (2019) Inorganic polyphosphate, a multifunctional polyanionic protein scaffold. J Biol Chem 294: 2180–2190

Yoo NG, Dogra S, Meinen BA, Tse E and others (2018) Polyphosphate stabilizes protein unfolding intermediates as soluble amyloid-like oligomers. J Mol Biol 430: 4195–4208

Yu J, Ding S, Zhong J, Fan C and others (2017) Evaluation of simulated dredging to control internal phosphorus release from sediments: focused on phosphorus transfer and resupply across the sediment–water interface. Sci Total Environ 592:662–673

Zak D, Gelbrecht J (2007) The mobilisation of phosphorus, organic carbon and ammonium in the initial stage of fen rewetting (a case study from NE Germany). Biogeochemistry 85:141–151

Zhou A, Tang H, Wang D (2005) Phosphorus adsorption on natural sediments: modeling and effects of pH and sediment composition. Water Res 39:1245–1254

Editorial responsibility: Robinson Fulweiler, Boston, Massachusetts, USA
Reviewed by: A. Schramm, E. Ingall and 1 anonymous referee

Submitted: May 4, 2022
Accepted: November 4, 2022
Proofs received from author(s): December 4, 2022